

1 **Characterization of Glycosylphosphatidylinositol Biosynthesis Defects**
2 **by Clinical Features, Flow Cytometry, and Automated Image Analysis**

3

4 Alexej Knaus^{1,2,3,4}, Jean Tori Pantel¹, Manuela Pendziwiat⁵, Nurulhuda Hajjir¹, Max Zhao¹,
5 Tzung-Chien Hsieh^{1,4}, Max Schubach^{1,6}, Yaron Gurovich⁷, Nicole Fleischer⁷, Marten Jäger^{1,6},
6 Sebastian Köhler¹, Hiltrud Muhle⁵, Christian Korff⁸, Rikke Steensbjerre Møller⁹, Allan
7 Bayat⁹, Patrick Calvas¹⁰, Nicolas Chassaing¹⁰, Hannah Warren¹¹, Steven Skinner¹¹; Raymond
8 Louie¹¹, Christina Evers¹², Marc Bohn¹³, Hans-Jürgen Christen¹⁴, Myrthe van den Born¹⁵,
9 Ewa Obersztyn¹⁶, Agnieszka Charzewska¹⁶, Milda Endziniene¹⁷, Fanny Kortüm¹⁸, Natasha
10 Brown^{19,20}, Peter N Robinson²¹, Helenius J Schelhaas²², Yvonne Weber²³, Ingo Helbig^{4,24},
11 Stefan Mundlos^{1,2}, Denise Horn^{1,25}, Peter M Krawitz^{1,2,4,25}

12

13 ¹ Institut für Medizinische Genetik und Humangenetik, Charité Universitätsmedizin Berlin,
14 13353 Berlin, Germany

15 ² Max Planck Institute for Molecular Genetics, 14195 Berlin, Germany

16 ³ Berlin-Brandenburg School for Regenerative Therapies, Charité Universitätsmedizin Berlin,
17 13353 Berlin, Germany

18 ⁴ Institute for Genomic Statistics and Bioinformatics, University Hospital Bonn, Rheinische
19 Friedrich-Wilhelms-Universität Bonn, 53127 Bonn, Germany

20 ⁵ Department of Neuropediatrics, University Medical Center Schleswig Holstein, 24105 Kiel,
21 Germany

22 ⁶ Berlin Institute of Health (BIH), 10178 Berlin, Germany

23 ⁷ FDNA, MA 02111 Boston, USA

24 ⁸ Unité de Neuropédiatrie, Université de Genève, CH-1211 Genève, Switzerland

25 ⁹ Department of Pediatrics, University Hospital of Hvidovre, 2650 Hvidovre, Denmark

26 ¹⁰ Service de Génétique Médicale, Hôpital Purpan, CHU, 31059 Toulouse, France

2

27 ¹¹ Greenwood Genetic Center, SC29646 Greenwood, USA

28 ¹² Genetische Poliklinik, Universitätsklinik Heidelberg, 69120 Heidelberg Germany

29 ¹³ St. Bernward Krankenhaus, 31134 Hildesheim, Germany

30 ¹⁴ Kinderkrankenhaus auf der Bult, Hannoversche Kinderheilstalt, 30173 Hannover,
31 Germany

32 ¹⁵ Department for Clinical Genetics, Erasmus MC, 3000 Rotterdam, Netherlands

33 ¹⁶ Institute of Mother and Child Department of Molecular Genetics, 01-211 Warsaw, Poland

34 ¹⁷ Neurology Department, Lithuanian University of Health Sciences, 50009 Kaunas, Lithuania

35 ¹⁸ Institute of Human Genetics, University Medical Center Hamburg-Eppendorf, 20246
36 Hamburg, Germany

37 ¹⁹ Victorian Clinical Genetics Services, Royal Children's Hospital, MCRI, Parkville,
38 Australia

39 ²⁰ Department of Clinical Genetics, Austin Health, Heidelberg, Australia

40 ²¹ The Jackson Laboratory for Genomic Medicine, 06032 Farmington, USA

41 ²² Departement of Neurology, Academic Center for Epileptology, 5590 Heeze, The
42 Netherlands

43 ²³ Department of Neurology and Epileptology and Hertie Institute for Clinical Brain Research,
44 University Tübingen, 72076 Tübingen Germany

45 ²⁴ Pediatric Neurology, Children's Hospital of Philadelphia, 3401 Philadelphia, USA

46 ²⁵ These authors contributed equally to this work and are co-senior authors

47

48 Correspondence to:

49 Denise Horn or Peter Krawitz: denise.horn@charite.de, pkrawitz@uni-bonn.de

50 Phone: 0049 30 450569132, Fax: 0049 30 45056991

51

52 **ABSTRACT**

53 **Background:** Glycosylphosphatidylinositol Biosynthesis Defects (GPIBDs) cause a group of
54 phenotypically overlapping recessive syndromes with intellectual disability, for which
55 pathogenic mutations have been described in 16 genes of the corresponding molecular
56 pathway. An elevated serum activity of alkaline phosphatase (AP), a GPI-linked enzyme, has
57 been used to assign GPIBDs to the phenotypic series of Hyperphosphatasia with Mental
58 Retardation Syndrome (HPMRS) and to distinguish them from another subset of GPIBDs,
59 termed Multiple Congenital Anomalies Hypotonia Seizures syndrome (MCAHS). However,
60 the increasing number of individuals with a GPIBD shows that hyperphosphatasia is a
61 variable feature that is not ideal for a clinical classification.

62 **Methods:** We studied the discriminatory power of multiple GPI-linked substrates that were
63 assessed by flow cytometry in blood cells and fibroblasts of 39 and 14 individuals with a
64 GPIBD, respectively. On the phenotypic level, we evaluated the frequency of occurrence of
65 clinical symptoms and analyzed the performance of computer-assisted image analysis of the
66 facial gestalt in 91 individuals.

67 **Results:** We found that certain malformations such as Morbus Hirschsprung and
68 Diaphragmatic defects are more likely to be associated with particular gene defects (*PIGV*,
69 *PGAP3*, *PIGN*). However, especially at the severe end of the clinical spectrum of HPMRS,
70 there is a high phenotypic overlap with MCAHS. Elevation of AP has also been documented
71 in some of the individuals with MCAHS, namely those with *PIGA* mutations. Although the
72 impairment of GPI-linked substrates is supposed to play the key role in the pathophysiology
73 of GPIBDs, we could not observe gene-specific profiles for flow cytometric markers or a
74 correlation between their cell surface levels and the severity of the phenotype. In contrast, it
75 was facial recognition software that achieved the highest accuracy in predicting the disease-
76 causing gene in a GPIBD.

77 **Conclusions:** Due to the overlapping clinical spectrum of both, HPMRS and MCAHS, in the
78 majority of affected individuals, the elevation of AP and the reduced surface levels of GPI-
79 linked markers in both groups, a common classification as GPIBDs is recommended. The
80 effectiveness of computer-assisted gestalt analysis for the correct gene inference in a GPIBD
81 and probably beyond is remarkable and illustrates how the information contained in human
82 faces is pivotal in the delineation of genetic entities.

83 **Key words:** GPI-anchor biosynthesis defects - automated image analysis - gene-prediction

84

85 **Background**

86 Inherited deficiencies of the glycosylphosphatidylinositol (GPI) biosynthesis are a
87 heterogeneous group of recessive Mendelian disorders that all share a common feature: The
88 function of GPI-linked proteins is compromised due to a defect in the GPI-anchor synthesis or
89 modification. Most of the enzymes involved in this molecular pathway are known and the
90 biochemical steps are well described [1]. With respect to the effect of genetic mutations on
91 the anchor and the GPI-linked substrate, several subdivisions of the pathway have been in use:
92 1) Early GPI-anchor synthesis, 2) Late GPI-anchor synthesis, 3) GPI transamidase, and 4)
93 Remodeling of fatty acids of the GPI-anchor after attachment to proteins (Figure S1).

94 The last two groups are defined by their molecular actions and comprise the genes *GPAAL1*,
95 *PIGK*, *PIGU*, *PIGS*, and *PIGT*, for the GPI-transamidase and *PGAP1*, *PGAP2*, *PGAP3*,
96 *MPPE1*, and *TMEM8* for the fatty acid remodeling. The differentiation between early and late
97 GPI-anchor synthesis considers the molecular consequence of the GPIBD and it was
98 suggested after an important finding from Murakami *et al.*, regarding the release of alkaline
99 phosphatase (AP) – a GPI-anchored marker [2]: If the anchor synthesis is stuck at an earlier
100 step, the transamidase does not get active and the hydrophobic signal peptide of GPI-anchor
101 substrates is not cleaved. As soon as the first mannose residue on the GPI-anchor has been
102 added by *PIGM*, the transamidase tries to attach the substrate to the anchor. However, if
103 subsequent steps are missing, the GPI-anchored proteins (GPI-APs) might be less stable and
104 hyperphosphatasia was hypothesized to be a consequence thereof.

105 The activity of the AP was regarded as such a discriminatory feature that it resulted in the
106 phenotypic series HPMRS 1 to 6, comprising currently the six genes *PGAP2*, *PGAP3*, *PIGV*,
107 *PIGO*, *PIGW* and *PIGY* [3-9]. Whenever a pathogenic mutation was discovered in a new gene
108 of the GPI-pathway and the developmentally delayed individuals showed an elevated AP in
109 the serum, the gene was simply added to this phenotypic series. If hyperphosphatasia was
110 missing, the gene was linked to another phenotypic series, Multiple Congenital Anomalies-

111 Hypotonia-Seizures (MCAHS) that currently consists of *PIGA*, *PIGN*, and *PIGT* [10-12].
112 However, the convention of dividing newly discovered GPIBDs over these two phenotypic
113 subgroups is only reasonable if they really represent distinguishable entities. This practice is
114 now challenged by a growing number of exceptions. The expressivity of most features is
115 variable and even the AP seems to be a biomarker with some variability: Some individuals
116 with mutations in *PIGA* also show elevated AP levels [10, 13-15], and some individuals with
117 mutations in *PIGO*, *PGAP2* and *PGAP3* show AP levels that are only borderline high [16-19].
118 Recently, deleterious mutations were identified in *PIGC*, *PIGP* and *PIGG* in individuals with
119 intellectual disability (ID), seizures and muscular hypotonia, but other features were missing
120 that were considered to be a prerequisite for MCAHS or HPMRS [20-22]. Despite of the large
121 phenotypic overlap with most GPIBDs, a flow cytometric analysis of granulocytes in
122 individuals with *PIGG* mutations did not show reduced surface levels for GPI-APs [20-22].
123 However, in the meantime, Zhao *et al.* could show that an impairment of *PIGG* in fibroblasts
124 affects the marker expression, indicating that there might also be variability depending on the
125 tissue [23]. In concordance with these finding also a case report of an individual with ID and
126 seizures that has mutations in *PIGQ*, seems a suggestive GPIBD, in spite of negative FACS
127 results [24].
128 The work of Markythanasis *et al.* can also be considered as a turning point in the naming
129 convention of phenotypes that are caused by deficiencies of the molecular pathway as OMIM
130 started now referring to them as a GPIBD (see OMIM entry #610293 for a discussion). In this
131 work we go one step further in this direction and ask the question whether also the phenotypic
132 series MCAHS and HPMRS should be abandoned in favor of a more gene-centered
133 description of the phenotype, which would also be in accordance with what Jaeken already
134 suggested for other congenital disorders of glycosylation [25]. Referring to GPIBD
135 phenotypes in a gene-specific manner makes particular sense if the gene can be predicted
136 from the phenotypic level with some accuracy. For this purpose, we analyzed systematically

137 the discriminatory power for GPIBDs for previously reported individuals as well as 23 novel
138 cases that were identified in routine diagnostics. This also adds in total novel FACS results of
139 16 patients on blood or fibroblasts, as well as 19 novel mutations (Figure S2).

140 Apart from founder effects that explain the reoccurrence of certain mutations with higher
141 frequency, pathogenic mutations have now been reported in many exons (Figure S2).
142 However, not much is known about genotype-phenotype correlations in these genes, which
143 makes bioinformatics interpretation of novel variants challenging. The phenotypic analysis,
144 for which we received ethics approval from the Charité University and obtained informed
145 consent from the responsible persons on behalf of all study participants, is based on three
146 different data sources, that is 1) a comprehensive clinical description of the phenotypic
147 features in HPO-terminology [26], 2) flow-cytometric profiles of multiple GPI-linked
148 markers, and 3) computer-assisted pattern recognition on frontal photos of individuals with a
149 molecularly confirmed diagnosis.

150 The rationale behind flow cytometry and image analyses is that GPIBDs might differ in their
151 effect on GPI-APs and their trafficking pathways, resulting in distinguishable phenotypes.
152 Interestingly, we found that the facial gestalt was well suited for a delineation of the
153 molecular entity. The high information content of the facies has become accessible just
154 recently by advanced phenotypic tools that might also be used for the analysis of other
155 pathway disorders. Before we present the results of flow cytometry and of automated image
156 analysis we will review the most important phenotypic features of GPIBDs in the old schema
157 of phenotypic series HPMRS and MCAHS.

158

159 **Methods and Study design**

160 **Clinical overview of HPMRS** Hyperphosphatasia with Mental Retardation Syndrome, which
161 is also sometimes referred to as Mabry syndrome (HPMRS1-6: MIM 239300, MIM 614749,
162 MIM 614207, MIM 615716, MIM 616025, MIM 616809), could present as an apparently

163 non-syndromic form of ID at one end of the clinical spectrum but also as a multiple
164 congenital malformation syndrome at the other end (Table S1). The distinct pattern of facial
165 anomalies of Mabry syndrome consist of wide set eyes, often with a large appearance and
166 upslanting palpebral fissures, a short nose with a broad nasal bridge and tip, and a tented
167 upper lip. The results of a computer-assisted comparison of the gene-specific facial gestalt
168 will be given in a later section.

169 Psychomotor delay, ID and variable AP elevation are the only consistent features of all
170 individuals with pathogenic mutations in *PIGV* [9, 27-33], *PIGO* [7, 16, 17, 30, 34-36],
171 *PGAP2* [4, 8, 18, 37], *PGAP3* [5, 19, 38-40], *PIGW* [3, 41], and *PIGY* [6]. Speech
172 development, especially expressive language, is more severely affected than motor skills in
173 the majority of the affected individuals (Table S1). Absent speech development was observed
174 in more than half of the affected individuals. Speech difficulties may be complicated by
175 hearing loss, which is present in a minority of affected individuals. In the different genetic
176 groups, seizures of various types and onset are present in about 65% of affected individuals.
177 Most affected individuals show a good response to anticonvulsive drugs, however, a few
178 affected individuals are classified as drug resistant and represent the clinically severe cases
179 (individual 14-0585). Muscular hypotonia is common in all types of HPMRS (about 65%).
180 Behavioral problems, in particular sleep disturbances and autistic features, tend to be frequent
181 (87%) in affected individuals with *PGAP3* mutations and are described in a few affected
182 individuals with *PIGY* mutations but are not documented in affected individuals with
183 mutations in the other four genes. Furthermore, ataxia and unsteady gait have been
184 documented in almost half of the affected individuals carrying *PGAP3* mutations and about a
185 third of this group did not achieve free walking at all.

186 Elevated values of AP were the key finding in affected individuals. However, a few cases are
187 documented with only minimal elevation of this parameter. The degree of persistent
188 hyperphosphatasia in the reported affected individuals varies over a wide range between about

189 1.1 and 17 times the age-adjusted upper limit of the normal range. The mean elevation of AP
190 is about 5 to 6 times the upper limit. Measurements at different ages of one individual show
191 marked variability of this value, for example from two times to seven times the upper limit.
192 There is no association between the AP activity and the degree of neurological involvement.
193 Furthermore, there is no correlation between the mutation class and genes with the level of
194 elevation of AP.

195 Growth parameters at birth are usually within the normal range. Most affected individuals
196 remain in the normal range although there is evidence of a skewed distribution towards the
197 upper centiles and a few affected individuals become overweight. In contrast, about 10% of
198 the affected individuals develop postnatal short stature and fail to thrive. About 27% of
199 affected individuals develop microcephaly, whereas less than 10% become macrocephalic.
200 Abnormalities of growth and head size do not correlate with a specific mutation or gene
201 within this group of genes.

202 Involvement of other organ systems varies among the genetically different groups. *PIGV*,
203 *PIGO*, and *PGAP2* affected individuals frequently suffer from a variety of different
204 malformations. Anorectal malformations, such as anal atresia or anal stenosis, are the most
205 frequent anomalies with almost 40% penetrance in the group of affected individuals. The
206 second most frequent anomaly is Hirschsprung disease with a frequency of about 25% in the
207 same group of affected individuals. Vesicoureteral or renal malformations occur with a
208 similar frequency, among them are congenital hydronephrosis, megaureter, and vesicoureteral
209 reflux. Our data revealed a frequency of heart defects of 20% in the group of affected
210 individuals with *PIGV*, *PIGO*, and *PGAP2* mutations, however, the type of cardiac
211 abnormality is variable. Only 2 of 26 affected individuals carrying *PGAP3* mutations have
212 variable congenital heart defects. Cleft palate is the malformation with the highest frequency
213 in the group of affected individuals with *PGAP3* mutations with a prevalence of almost 60%,
214 whereas other malformations are rarely observed. Exceptional is a group of 10 Egyptian

215 individuals with the same founder mutation and a high incidence of structural brain anomalies
216 (thin corpus callosum (8/10), vermis hypoplasia (4/10), ventriculomegaly (3/10) and Dandy-
217 Walker malformation (1/10) [28, 38]. Up to date these are the few individuals with a
218 presumable complete loss of function for this gene (NM_033419.3:c.402dupC,
219 p.Met135Hisfs*28; c.817_820 delGACT, p.Asp273Serfs*37)).

220 Malformations had not been observed in the single reported affected individual with *PIGW*
221 mutations [3]. Apart from dilation of renal collecting systems, affected individuals with *PIGY*
222 mutations presented with a new spectrum of organ involvement such as cataracts, rhizomelic
223 shortness of limbs, contractures and hip dysplasia [6].

224 All affected individuals with *PIGV* and *PIGO* mutations had a variable degree of distal hand
225 anomalies, namely brachytelephalangy. They showed hypoplastic finger nails as well as
226 hypoplastic distal phalanges in the hand X-rays. Often, they displayed broad and short distal
227 phalanges of the thumbs and halluces including short and broad corresponding nails of the
228 affected digits. Brachytelephalangy is not present in any of the affected individuals with
229 *PGAP3*, *PGAP2* and *PIGW* mutations, respectively, although one third showed broad nails
230 without radiological abnormalities in the available X-rays. One of four affected individuals
231 with *PIGY* mutations showed brachytelephalangy.

232 A multidisciplinary approach is required to manage the GPIBDs described in this section, as
233 the clinical variability is broad. It is recommended that all affected individuals have at least
234 one baseline renal ultrasound investigation as well as an echocardiography to rule out any
235 obvious malformations. In case of chronic obstipation, Hirschsprung disease, as well as anal
236 anomalies should be excluded. Hearing evaluation is recommended in all affected individuals.

237 Individuals with behavioral problems may benefit from a review by a clinical psychologist.
238 Regular developmental assessments and EEG investigations are required to ensure that
239 affected individuals get optimal support. The tendency towards epilepsies has been reported to

240 decrease in some affected individuals with growing age and if the affected individual and
241 physician agree to a trial discontinuation of therapy, medications could be tapered.

242

243 **Clinical overview of MCAHS:** MCAHS comprises a group of genetically different disorders
244 characterized by early onset forms of different types of epilepsies with poor prognosis,
245 missing or minimal psychomotor development and often, early death (Table S2). The
246 phenotypic series include individuals with *PIGA* (MIM 300868)[10, 13-15, 42-46], *PIGN*
247 (MIM 614080)[12, 18, 47-53], and *PIGT* (MIM 615398)[11, 39, 54-57] mutations.

248 Neonatal muscular hypotonia is often present. The variable congenital anomalies affect the
249 renal/vesicoureteral, cardiac and gastrointestinal systems. Brain imaging showed variable
250 abnormalities, for example thin corpus callosum, cerebellar atrophy/hypoplasia, cerebral
251 atrophy and delayed myelination but also normal findings in other affected individuals. The
252 spectrum of malformations is overlapping with that of HPMRS apart from megacolon, which
253 is only reported in *PIGV*, *PIGO*, and *PGAP2* positive individuals and diaphragmatic defects,
254 which are only documented in three fetuses with *PIGN* mutations [51]. In addition, joint
255 contractures and hyperreflexia are documented in some individuals with *PIGA* and *PIGN*
256 mutations [10, 13-15, 42-46]. Macrocephaly or macrosomia occur in some of these
257 individuals, whereas microcephaly occurs in others. No distinct facial phenotype is
258 recognizable in comparison within and between the genetically different groups of MCAHS.

259 Interestingly, 5 out of 23 individuals with *PIGA* mutations had elevated AP measurements,
260 whereas only one individual with *PIGN* mutations was reported with borderline high AP
261 activity [52]. In contrast, some of the individuals with *PIGT* mutations showed decreased AP
262 [11, 39, 54, 57].

263 HPMRS and MCAHS display an overlapping clinical spectrum but with a considerably worse
264 prognosis in MCAHS due to early onset and often intractable seizures as well as early death
265 in the majority of affected individuals. However, facial dysmorphisms do not appear to be

266 characteristic in the different types of MCAHS in contrast to HPMRS. Importantly, elevation
267 of AP and reduced surface levels of GPI linked substrates are not restricted to HPMRS.

268 **Flow cytometry**

269 Flow cytometry analysis of blood:

270 Flow cytometry was performed on granulocytes extracted from peripheral blood draws that
271 were sampled in BCT CytoChex tubes (Streck, USA, NE), shipped and analyzed in less than
272 72 hours. 50µl whole blood were mixed with 20µl of an antibody panel:

273 1. 4µl CD55-PE (BD #555694), 4µl CD59-FITC (BD #555763), 2µl CD45-PacBlue
274 (Beckman Coulter, clone J.33) and 10µl FACS buffer.

275 2. 2µl CD16-PE (Beckman Coulter, clone 3G8), 4µl FLAER-AF488 (FL2S-C;
276 Burlington, Canada,), 2µl CD45-PacBlue (Beckman Coulter, clone J.33) and 12µl
277 FACS buffer.

278 3. 2µl CD24-APC (MiltenyiBiotec Clone REA832) 2µl CD45-PacBlue (Beckman
279 Coulter, clone J.33) and 16µl FACS buffer.

280 The staining was incubated for 30 min at room temperature followed by an incubation with
281 500µl red blood cell lysis buffer for 10min. Debris was removed by discarding the
282 supernatant after centrifugation, the cell pellet was washed twice with 200µl, and resuspended
283 in 100µl FACS buffer for flow cytometry analysis on a MACSQuant VYB (MiltenyiBiotec,
284 Bergisch Gladbach, Germany).

285 Gating for living cells was based on forward and side scatter (FSC-A vs. SSC-A). Single cells
286 were gated on a diagonal (FSC-A vs. FSH-H). Granulocytes were identified as granular (SSC-
287 A high) and CD45 positive cells.

288 The reduction of GPI-AP expression was assessed by the ratio of the median fluorescence
289 intensity (MFI) of the patient to the MFI of a shipped healthy control. Heterozygous carriers
290 of pathogenic mutations (parents) were used as controls when unrelated healthy controls were
291 not available. It is noteworthy that differences in GPI-AP expression were subtle in healthy

292 parents compared to unrelated controls. To compare marker reduction of published and
293 unpublished cases only FLAER and CD16 were used.

294

295 Flow cytometric analysis of fibroblast cells:

296 Fibroblasts derived from skin biopsies of patients, parents and healthy control individuals
297 were cultured in DMEM supplemented with 10% FCS, 1% Ultraglutamine, 1% Penicillin /
298 Streptomycin. For flow cytometry analysis confluent grown cells were washed twice with
299 PBS (-Ca²⁺, -Mg²⁺), cells were gently detached from the coulter dish with Trypsin-EDTA
300 (0.01%). The single cell suspension was washed with FACS buffer, counted, diluted (100.000
301 cells / stain), centrifuged, supernatant was discarded, and the cell pellet was resuspended in
302 the following antibody mix.

- 303 1. 4µl CD55-PE (BD #555694), 4µl CD59-FITC (BD #555763), and 12µl FACS buffer.
304 2. 4µl CD73-PE (BD#550257) 4µl FLAER-AF488 (Cedarlane, FL2S-C), and 12µl
305 FACS buffer.

306 The staining was incubated for 30min at room temperature followed by two washing steps
307 with 200µl FACS buffer. For flow cytometry analysis on a MACSQuant VYB the cells were
308 resuspended in 100µl FACS buffer.

309 Reduction of GPI-AP expression was calculated as a ration between the median fluorescence
310 intensity (MFI) of the patient against the mean of MFIs from healthy parents and a healthy
311 unrelated control. It is noteworthy that heterozygous carriers of pathogenic mutations
312 (parents) and unrelated healthy controls had only subtle differences in GPI-AP expression.

313

314 **Computer-assisted phenotype comparison**

315 Facial images of all individuals with a molecularly confirmed GPIBD were assessed with the
316 Face2Gene Research Application (FDNA Inv., Boston MA, USA). This software tool set
317 allows the phenotypic comparison of user-defined cohorts with ten or more individuals. The

318 classification model of Face2Gene Research uses a neural network architecture that consists
319 of ten convolutional layers, each but the last followed by batch normalization [Gurovich, et
320 al.]. The original collections are split into train/test sets for cross-validation and mean
321 accuracies for the classification process are computed. The result of a single experiment is a
322 confusion matrix that describes the performance of the classification process. As cohort size is
323 a known confounder, we randomly sampled all cohorts down to the same size (n=10) and
324 computed the mean true positive and error rates as well as the standard deviation from ten
325 iterations. The scripts for the simulations are available on request and can be used to
326 reproduce the results.

327

328 **Results**

329 **Flow cytometric assessment of GPIBDs**

330 We acquired fibroblast cultures of affected individuals to perform the measurements under the
331 same experimental conditions repeatedly. The marker FLAER that binds to the GPI-anchor
332 directly, as well as the GPI-APs CD55, CD59, and CD73 that show high expression levels on
333 fibroblasts were assessed (Figure 1). We hypothesized that measuring cell surface levels of
334 GPI-linked substrates directly by flow cytometry might be more suitable to quantify the
335 severity of a GPIBD or to predict the affected gene. No significant difference between
336 patients with MCAHS was observed compared to patients with HPMRS (Figure 1a).
337 Furthermore, the cell surface levels of CD55 and CD59 were in average lower in cells that
338 were derived from individuals with mutations in *PGAP3* compared to individuals with
339 mutations in *PIGV* (Table S3), although this did not correspond to a higher prevalence to
340 seizures or a more severe developmental delay. CD55 and CD59 are of particular interest as
341 they protect cells from an attack of the activated complement system and the membrane attack
342 complex that has also been shown to be involved in the pathogenesis of seizures [58].

343 The samples with pathogenic mutations in *PIGV* are noteworthy as they are derived from
344 individuals that differ considerably in the severity of their phenotype: 14-0585 was born with
345 multiple malformations and his seizures are resistant to treatment, whereas the other three
346 individuals A2, A3, and P1 are considered as moderately affected. The flow cytometric
347 profiles, however, do not show marked differences. Furthermore, the cell surface levels of
348 CD55 and CD59 were in average lower in cells that were derived from individuals with
349 mutations in *PGAP3*.

350 While the reproducibility of the flow cytometric data on fibroblasts is attractive, the small size
351 of the sample set is clearly a disadvantage in the assessment of potential differences between
352 the phenotypic subgroups of GPIBDs. Most flow cytometric analyses have been performed on
353 granulocytes of affected individuals with the markers CD16 and FLAER and we added a
354 comparison of the relative median fluorescent intensities (rMFI) for altogether 39 individuals
355 of the phenotypic series MCAHS and HPMRS (Table S4). Although individuals of the
356 MCAHS spectrum are usually more severely affected than individuals of the HPMRS
357 spectrum, we did not observe any significant differences for the tested markers (Figure 1 B).
358 Thus, no significant correlation between FACS profiles of the two phenotypic series was
359 found.

360

361 **Comparison of the facial gestalt of GPIBDs**

362 The craniofacial characteristics of many Mendelian disorders are highly informative for
363 clinical geneticists and have also been used to delineate gene-specific phenotypes of several
364 GPIBDs [3-5, 10, 19, 27-29, 31, 38, 39, 43, 44, 59-61]. However, our medical terminology is
365 often not capable of describing subtle differences in the facial gestalt. Therefore, computer-
366 assisted analysis of the gestalt has recently received much attention in syndromology and
367 several groups have shown that the clinical face phenotype space (CFPS) can also be
368 exploited by machine learning approaches [62]. If a recognizable gestalt exists, a classifier for

369 facial patterns can be trained to infer likely differential diagnoses. Conversely, if photos of
370 affected individuals with disease-causing mutations in different genes of a pathway form
371 separate clusters, it indicates that the gestalt is distinguishable to a certain extent. FDNA's
372 recently launched RESEARCH application is a deep learning tool for exactly this purpose
373 (<https://app.face2gene.com/research>): A classification model is generated on two or more
374 collections of frontal images and the performance is reported in means of a confusion matrix.
375 If true positive rates for the single gene-phenotypes are achieved that are significantly better
376 than for a random assignment of photos to cohorts, there is some phenotypic substructure and
377 the null-hypothesis of perfect heterogeneity may be rejected.

378 We used the RESEARCH app of the Face2Gene suite to evaluate a classifier for the five most
379 prevalent GPIBDs, that is *PIGA* (n=20), *PIGN* (n=11), *PIGT* (n=12), *PIGV* (n=25), and
380 *PGAP3* (n=23) at the current moment. Our original sample set thus consists of frontal facial
381 photos of 91 individuals with a molecularly confirmed diagnosis of HPMRS or MCAHS,
382 including cases that have been previously published [5, 9-11, 13-15, 19, 27-29, 31-33, 38, 43,
383 47, 49, 50, 52-56, 60, 63]. The mean accuracy that is achieved on this original sample set is
384 52.2 %, which is significantly better than randomly expected. In order compare the
385 performances for the single gene classes we had to exclude confounding effects from
386 unbalanced cohort sizes and sampled the cohorts down to the same size of $n=10$. Although
387 this decreases the overall performance, the mean accuracy of 45.8% is still significantly better
388 than the 20% that would be achieved by chance in a 5-class-problem for evenly sized cohorts
389 (Figure 2). Furthermore, for every single gene-phenotype, the true positive rate (TPR) was
390 better than randomly expected with *PIGV* achieving the highest value (59%).

391 Interestingly, we observed the highest false negative rate in the confusion matrix for *PGAP3*
392 (HPMRS4): In average these cases are erroneously classified as *PIGV* (HPMRS1) 32% of the
393 cases. This finding is in good agreement with the phenotypic delineation from
394 syndromologists that grouped these to genes in the same subclass. A cluster analysis of the

395 confusion matrix actually reproduces the two phenotypic series as shown by the dendrogram
396 in Figure 2.

397 While the confusion matrix on the entire sample set can be used to decide whether there are
398 gene-specific substructures in the GPI-pathway, pairwise comparisons are better suited to
399 workup phenotypic differences between genes even inside a phenotypic series. We therefore
400 evaluated the area under the receiver operating characteristics curve (AUC) and found the
401 correct gene-prediction more often than randomly expected, including *PIGV* versus *PGAP3*
402 (Figure S3). The differences in pair-wise comparison between *PIGV* and *PGAP3* could be
403 confounded by the large number of Egyptian cases in the *PGAP3* cohort [38], the effect of
404 which we could not further analyze due to the limited set of patients photos.

405

406 **Discussion**

407 The identification of multiple affected individuals with GPIBDs has enabled the analysis of
408 genotype-phenotype relationships for the molecular pathway of GPI anchor synthesis. Besides
409 a developmental delay and seizures, which are common findings in most affected individuals
410 with a GPIBD, the clinical variability and the variation in expressivity is wide. So far,
411 recognizable gene-specific phenotypes seem to be accepted for *PIGL* and are discussed for
412 *PIGM* [64, 65]. For other GPIBDs the phenotypic series HPMRS and MCAHS have been
413 used to subgroup the pathway and the activity of the AP in the serum was the main
414 classification criterion. However, these disease entities are increasingly cumbersome as some
415 cases are now known that do not go along with this oversimplified rule.

416 We therefore compared GPIBDs based on deep phenotyping data and flow cytometric profiles
417 of GPI-APs. Among the 16 genes of the GPI pathway with reports of affected individuals,
418 mutations in *PIGA*, *PIGN*, *PIGT*, *PIGV*, and *PGAP3* were most numerous and these GPIBDs
419 were also suitable for an automated image analysis.

420 A systematic evaluation of the phenotypic features showed that certain malformations occur
421 with a higher frequency in specific GPIBDs. To date, megacolon has only been found to be
422 associated with *PIGV*, *PIGO*, and *PGAP2* mutations. Diaphragmatic defects have only been
423 documented in affected individuals with *PIGN* mutations. Only in individuals with *PGAP3*
424 mutations, behavioral problems, especially sleep disturbances and autistic features, are present
425 in about 90%. In addition, ataxia and unsteady gait are also frequently documented in this
426 group but not in the others. An accurate classification that is merely based on clinical
427 symptoms is, however, not possible due to their high variability. Also, flow cytometric
428 analysis of GPI-marker expressions were not indicative for the gene defect and did not
429 correlate with the severity of the phenotype. Of note is, however, that an assessment of the
430 GPI-AP expression levels seems more sensitive in the fibroblasts than in blood cells [23].
431 This might also be related to the trafficking pathways of GPI-APs through ER and Golgi that
432 differ for cell types and substrates [66, 67].

433 The overlapping clinical spectrum of both, HPMRS and MCAHS, the findings of elevated AP
434 and the reduced surface levels of GPI linked proteins in some of the MCAHS cases favor a
435 common classification as GPIBDs.

436 In light of the high variability and expressivity of the clinical findings and the weak genotype-
437 phenotype correlation, the most surprising finding of our study was the high discriminatory
438 power that facial recognition technology achieved. In spite of the similarity of the
439 pathophysiology, differences in the gestalt are still perceptible. This illustrates the remarkable
440 information content of human faces and advocates for the power of computer-assisted
441 syndromology in the definition of disease entities.

442 Automated image analysis of syndromic disorders is a comparably new field of research and
443 the approach that we used requires photos of at least ten individuals per cohort. However, it is
444 currently not known if there is a minimum number of cases that is required to assess whether
445 a gene-phenotype is recognizable. Furthermore, for every rare disorder with a characteristic

446 gestalt there is possibly a maximum value for the recognizability. So far, the approximation of
447 this upper limit has not systematically been studied depending on the number of individuals
448 that were used in the training process and should definitely be a focus for future research.

449

450 **Web resources**

451 <https://app.face2gene.com/research>

452

453 **Funding**

454 This work was supported by grants from the German Ministry of Research and Education to
455 M.S. (BMBF project number 01EC1402B), and the German Research Foundation to I.H. (HE
456 5415/6-1), Y.W. (WE 4896/3-1), and P.M.K (KR3985/7-3).

457

458 **Availability of data and materials**

459 All data that was used for the phenotypic analysis is part of a larger effort, called DPDL, that
460 serves as a case-centered data collection for benchmarking of automated imaging technology.

461 Access to DPDL is available upon request. On Face2Gene registered users can rerun the
462 experiments for phenotypic comparison in the RESEARCH App:

463 <https://app.face2gene.com/research>

464

465 **Competing interests**

466 PMK is member of the scientific advisory board of FDNA.

467

468 **Figure legends:**

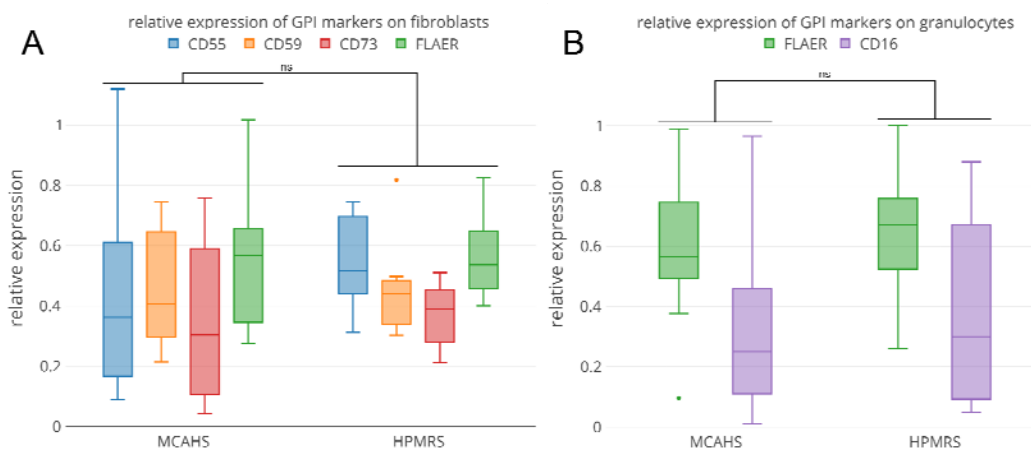
469 **Figure 1: Flow cytometric profiling for GPIBDs:** Cell surface levels of FLAER and tissue
470 specific GPI-anchored proteins were assessed on fibroblasts A) as well as on granulocytes B)
471 of individuals affected by GPIBDs. The relative expression was grouped for GPIBDs of the

472 same phenotypic series MCAHS (*PIGA*, *PIGN*, *PIGT*) and HPMRS (*PGAP3*, *PIGV*, *PIGO*,
473 *PIGW*) but showed no significant differences (significance was tested with Wilcoxon-Mann-
474 Whitney Test, the p-Value was corrected for sample size (Bonferoni)).

475

476 **Figure 2: Automated image analysis for five of the most prevalent GPIBDs.** A model for
477 the classification of the gene-phenotypes was repeatedly trained and cross-validated on patient
478 subsets that were randomly down-sampled to the same cohort size of n=10. A mean accuracy
479 of 0.44 was achieved which is significantly better than randomly expected (0.20). For
480 explanatory purposes, the rows of the confusion matrix start with instances of previously
481 published or newly identified individuals with GPIBDs. If the predicted gene matches the
482 molecularly confirmed diagnosis, such a test case would contribute to the true positive rate,
483 shown on the diagonal. Actual affected individual photographs were used to generate an
484 averaged and de-identified composite photo and are shown on top of the columns. The
485 performance of computer-assisted image classification is significantly better than expected
486 under the null model of perfect heterogeneity and indicates a gene-specific phenotypic
487 substructure for the molecular pathway disease. Higher false positive error rates occur
488 between genes of the same phenotypic series, HPMRS and MCAHS, as indicated by the
489 dendrogram.

490



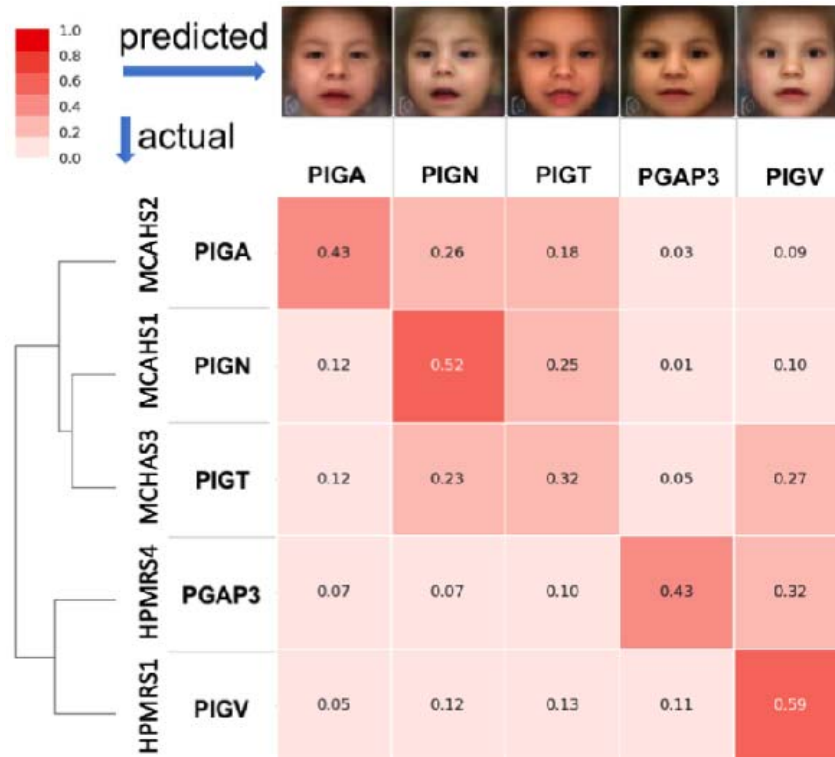
491

492

—

493 **Figure 1: Flow cytometric profiling for GPIBDs: Cell surface levels of FLAER and tissue specific GPI-anchored**
494 **proteins were assessed on $n=14$ fibroblasts A) as well as on $n=39$ granulocytes B) of individuals affected by GPIBDs.**
495 **The relative expression was grouped for GPIBDs of the same phenotypic series MCAHS (*PIGA*, *PIGN*, *PIGT*) and**
496 **HPMRS (*PGAP3*, *PIGV*, *PIGO*, *PIGW*) but showed no significant differences (significance was tested with Wilcoxon-**
497 **Mann-Whitney Test, the p-Value was corrected for sample size (Bonferoni).**

498



499

500

501

502

503

504

505

506

507

508

509

Figure 2: Automated image analysis for five of the most prevalent GPIBDs. A model for the classification of the gene-phenotypes was repeatedly trained and cross-validated on patient subsets that were randomly down-sampled to the same cohort size of $n=10$. A mean accuracy of 0.44 was achieved which is significantly better than randomly expected (0.20). For explanatory purposes, the rows of the confusion matrix start with instances of previously published or newly identified individuals with GPIBDs. If the predicted gene matches the molecularly confirmed diagnosis, such a test case would contribute to the true positive rate, shown on the diagonal. Actual affected individual photographs were used to generate an averaged and de-identified composite photo and are shown on top of the columns. The performance of computer-assisted image classification is significantly better than expected under the null model of perfect heterogeneity and indicates a gene-specific phenotypic substructure for the molecular pathway disease. Higher false positive error rates occur between genes of the same phenotypic series, HPMRS and MCAHS, as indicated by the dendrogram.

510

511 References

- 512 1. Kinoshita T, Fujita M, Maeda Y: **Biosynthesis, remodelling and functions of**
513 **mammalian GPI-anchored proteins: recent progress.** *Journal of biochemistry*
514 2008, **144**(3):287-294.
- 515 2. Murakami Y, Kanzawa N, Saito K, Krawitz PM, Mundlos S, Robinson PN,
516 Karadimitris A, Maeda Y, Kinoshita T: **Mechanism for release of alkaline**
517 **phosphatase caused by glycosylphosphatidylinositol deficiency in patients with**
518 **hyperphosphatasia-mental retardation syndrome.** *The Journal of biological*
519 *chemistry* 2012.
- 520 3. Chiyonobu T, Inoue N, Morimoto M, Kinoshita T, Murakami Y:
521 **Glycosylphosphatidylinositol (GPI) anchor deficiency caused by mutations in**
522 **PIGW is associated with West syndrome and hyperphosphatasia with mental**
523 **retardation syndrome.** *J Med Genet* 2014, **51**(3):203-207.
- 524 4. Hansen L, Tawamie H, Murakami Y, Mang Y, ur Rehman S, Buchert R, Schaffer S,
525 Muhammad S, Bak M, Nothen MM *et al*: **Hypomorphic mutations in PGAP2,**
526 **encoding a GPI-anchor-remodeling protein, cause autosomal-recessive**
527 **intellectual disability.** *American journal of human genetics* 2013, **92**(4):575-583.
- 528 5. Howard MF, Murakami Y, Pagnamenta AT, Daumer-Haas C, Fischer B, Hecht J,
529 Keays DA, Knight SJ, Kolsch U, Kruger U *et al*: **Mutations in PGAP3 Impair GPI-**
530 **Anchor Maturation, Causing a Subtype of Hyperphosphatasia with Mental**
531 **Retardation.** *American journal of human genetics* 2014.
- 532 6. Ilkovski B, Pagnamenta AT, O'Grady GL, Kinoshita T, Howard MF, Lek M, Thomas
533 B, Turner A, Christodoulou J, Sillence D *et al*: **Mutations in PIGY: expanding the**
534 **phenotype of inherited glycosylphosphatidylinositol (GPI) deficiencies.** *Hum Mol*
535 *Genet* 2015.
- 536 7. Krawitz PM, Murakami Y, Hecht J, Kruger U, Holder SE, Mortier GR, Delle Chiaie
537 B, De Baere E, Thompson MD, Roscioli T *et al*: **Mutations in PIGO, a member of**
538 **the GPI-anchor-synthesis pathway, cause hyperphosphatasia with mental**
539 **retardation.** *American journal of human genetics* 2012, **91**(1):146-151.
- 540 8. Krawitz PM, Murakami Y, Riess A, Hietala M, Kruger U, Zhu N, Kinoshita T,
541 Mundlos S, Hecht J, Robinson PN *et al*: **PGAP2 mutations, affecting the GPI-**
542 **anchor-synthesis pathway, cause hyperphosphatasia with mental retardation**
543 **syndrome.** *American journal of human genetics* 2013, **92**(4):584-589.
- 544 9. Krawitz PM, Schweiger MR, Rodelsperger C, Marcelis C, Kolsch U, Meisel C,
545 Stephani F, Kinoshita T, Murakami Y, Bauer S *et al*: **Identity-by-descent filtering of**
546 **exome sequence data identifies PIGV mutations in hyperphosphatasia mental**
547 **retardation syndrome.** *Nature genetics* 2010, **42**(10):827-829.
- 548 10. Johnston JJ, Gropman AL, Sapp JC, Teer JK, Martin JM, Liu CF, Yuan X, Ye Z,
549 Cheng L, Brodsky RA *et al*: **The phenotype of a germline mutation in PIGA: the**
550 **gene somatically mutated in paroxysmal nocturnal hemoglobinuria.** *American*
551 *journal of human genetics* 2012, **90**(2):295-300.
- 552 11. Kvarnung M, Nilsson D, Lindstrand A, Korenke GC, Chiang SC, Blennow E,
553 Bergmann M, Stodberg T, Makitie O, Anderlid BM *et al*: **A novel intellectual**
554 **disability syndrome caused by GPI anchor deficiency due to homozygous**
555 **mutations in PIGT.** *J Med Genet* 2013.
- 556 12. Maydan G, Noyman I, Har-Zahav A, Neria ZB, Pasmanik-Chor M, Yeheskel A,
557 Albin-Kaplanski A, Maya I, Magal N, Birk E *et al*: **Multiple congenital anomalies-**
558 **hypotonia-seizures syndrome is caused by a mutation in PIGN.** *Journal of medical*
559 *genetics* 2011, **48**(6):383-389.
- 560 13. Fauth C, Steindl K, Toutain A, Farrell S, Witsch-Baumgartner M, Karall D, Joset P,
561 Bohm S, Baumer A, Maier O *et al*: **A recurrent germline mutation in the PIGA**

- 562 **gene causes Simpson-Golabi-Behmel syndrome type 2. *Am J Med Genet A* 2016,
563 **170A(2):392-402.****
- 564 14. Kato M, Saitsu H, Murakami Y, Kikuchi K, Watanabe S, Iai M, Miya K, Matsuura R,
565 Takayama R, Ohba C *et al*: **PIGA mutations cause early-onset epileptic**
566 **encephalopathies and distinctive features.** *Neurology* 2014, **82(18):1587-1596.**
- 567 15. van der Crabben SN, Harakalova M, Brilstra EH, van Berkestijn FM, Hofstede FC,
568 van Vught AJ, Cuppen E, Kloosterman W, Ploos van Amstel HK, van Haaften G *et al*:
569 **Expanding the spectrum of phenotypes associated with germline PIGA**
570 **mutations: a child with developmental delay, accelerated linear growth, facial**
571 **dysmorphisms, elevated alkaline phosphatase, and progressive CNS**
572 **abnormalities.** *Am J Med Genet A* 2014, **164A(1):29-35.**
- 573 16. Nakamura K, Osaka H, Murakami Y, Anzai R, Nishiyama K, Kodera H, Nakashima
574 M, Tsurusaki Y, Miyake N, Kinoshita T *et al*: **PIGO mutations in intractable**
575 **epilepsy and severe developmental delay with mild elevation of alkaline**
576 **phosphatase levels.** *Epilepsia* 2014, **55(2):e13-17.**
- 577 17. Zehavi Y, von Renesse A, Daniel-Spiegel E, Sapir Y, Zalman L, Chervinsky I,
578 Schuelke M, Straussberg R, Spiegel R: **A homozygous PIGO mutation associated**
579 **with severe infantile epileptic encephalopathy and corpus callosum hypoplasia,**
580 **but normal alkaline phosphatase levels.** *Metab Brain Dis* 2017.
- 581 18. Jezela-Stanek A, Ciara E, Piekutowska-Abramczuk D, Trubicka J, Jurkiewicz E,
582 Rokicki D, Mierzewska H, Spsychalska J, Uhrynowska M, Szwarc-Bronikowska M *et*
583 *al*: **Congenital disorder of glycosylphosphatidylinositol (GPI)-anchor**
584 **biosynthesis--The phenotype of two patients with novel mutations in the PIGN**
585 **and PGAP2 genes.** *Eur J Paediatr Neurol* 2016, **20(3):462-473.**
- 586 19. Knaus A, Awaya T, Helbig I, Afawi Z, Pendziwiat M, Abu-Rachma J, Thompson
587 MD, Cole DE, Skinner S, Annese F *et al*: **Rare Noncoding Mutations Extend the**
588 **Mutational Spectrum in the PGAP3 Subtype of Hyperphosphatasia with Mental**
589 **Retardation Syndrome.** *Hum Mutat* 2016, **37(8):737-744.**
- 590 20. Edvardson S, Murakami Y, Nguyen TT, Shahrour M, St-Denis A, Shaag A, Damseh
591 N, Le Deist F, Bryceson Y, Abu-Libdeh B *et al*: **Mutations in the**
592 **phosphatidylinositol glycan C (PIGC) gene are associated with epilepsy and**
593 **intellectual disability.** *J Med Genet* 2017, **54(3):196-201.**
- 594 21. Johnstone DL, Nguyen TT, Murakami Y, Kernohan KD, Tetreault M, Goldsmith C,
595 Doja A, Wagner JD, Huang L, Hartley T *et al*: **Compound heterozygous mutations**
596 **in the gene PIGP are associated with early infantile epileptic encephalopathy.**
597 *Hum Mol Genet* 2017, **26(9):1706-1715.**
- 598 22. Makrythanasis P, Kato M, Zaki MS, Saitsu H, Nakamura K, Santoni FA, Miyatake S,
599 Nakashima M, Issa MY, Guipponi M *et al*: **Pathogenic Variants in PIGG Cause**
600 **Intellectual Disability with Seizures and Hypotonia.** *American journal of human*
601 *genetics* 2016, **98(4):615-626.**
- 602 23. Zhao JJ, Halvardson J, Knaus A, Georgii-Hemming P, Baeck P, Krawitz PM,
603 Thuresson AC, Feuk L: **Reduced cell surface levels of GPI-linked markers in a**
604 **new case with PIGG loss of function.** *Hum Mutat* 2017.
- 605 24. Martin HC, Kim GE, Pagnamenta AT, Murakami Y, Carvill GL, Meyer E, Copley
606 RR, Rimmer A, Barcia G, Fleming MR *et al*: **Clinical whole-genome sequencing in**
607 **severe early-onset epilepsy reveals new genes and improves molecular diagnosis.**
608 *Hum Mol Genet* 2014, **23(12):3200-3211.**
- 609 25. Jaeken J: **Congenital disorders of glycosylation (CDG): it's (nearly) all in it!** *J*
610 *Inherit Metab Dis* 2011, **34(4):853-858.**

- 611 26. Robinson PN, Kohler S, Bauer S, Seelow D, Horn D, Mundlos S: **The Human**
612 **Phenotype Ontology: a tool for annotating and analyzing human hereditary**
613 **disease**. *American journal of human genetics* 2008, **83**(5):610-615.
- 614 27. Horn D, Krawitz P, Mannhardt A, Korenke GC, Meinecke P: **Hyperphosphatasia-**
615 **mental retardation syndrome due to PIGV mutations: expanded clinical**
616 **spectrum**. *American journal of medical genetics Part A* 2011, **155A**(8):1917-1922.
- 617 28. Thompson MD, Roscioli T, Marcelis C, Nezarati MM, Stolte-Dijkstra I, Sharom FJ,
618 Lu P, Phillips JA, Sweeney E, Robinson PN *et al*: **Phenotypic variability in**
619 **hyperphosphatasia with seizures and neurologic deficit (Mabry syndrome)**.
620 *American journal of medical genetics Part A* 2012, **158A**(3):553-558.
- 621 29. Horn D, Wieczorek D, Metcalfe K, Baric I, Palezac L, Cuk M, Petkovic Ramadza D,
622 Kruger U, Demuth S, Heinritz W *et al*: **Delineation of PIGV mutation spectrum**
623 **and associated phenotypes in hyperphosphatasia with mental retardation**
624 **syndrome**. *Eur J Hum Genet* 2014, **22**(6):762-767.
- 625 30. Xue J, Li H, Zhang Y, Yang Z: **Clinical and genetic analysis of two Chinese infants**
626 **with Mabry syndrome**. *Brain Dev* 2016, **38**(9):807-818.
- 627 31. Reynolds KK, Juusola J, Rice GM, Giampietro PF: **Prenatal presentation of Mabry**
628 **syndrome with congenital diaphragmatic hernia and phenotypic overlap with**
629 **Fryns syndrome**. *Am J Med Genet A* 2017, **173**(10):2776-2781.
- 630 32. Rabe P, Haverkamp F, Emons D, Roskamp R, Zerres K, Passarge E: **Syndrome of**
631 **developmental retardation, facial and skeletal anomalies, and hyperphosphatasia**
632 **in two sisters: nosology and genetics of the Coffin-Siris syndrome**. *Am J Med*
633 *Genet* 1991, **41**(3):350-354.
- 634 33. Marcelis CL, Rieu P, Beemer F, Brunner HG: **Severe mental retardation, epilepsy,**
635 **anal anomalies, and distal phalangeal hypoplasia in siblings**. *Clin Dysmorphol*
636 2007, **16**(2):73-76.
- 637 34. Morren MA, Jaeken J, Visser G, Salles I, Van Geet C, BioResource N, Simeoni I,
638 Turro E, Freson K: **PIGO deficiency: palmoplantar keratoderma and novel**
639 **mutations**. *Orphanet J Rare Dis* 2017, **12**(1):101.
- 640 35. Kuki I, Takahashi Y, Okazaki S, Kawawaki H, Ehara E, Inoue N, Kinoshita T,
641 Murakami Y: **Vitamin B6-responsive epilepsy due to inherited GPI deficiency**.
642 *Neurology* 2013, **81**(16):1467-1469.
- 643 36. Tanigawa J, Mimatsu H, Mizuno S, Okamoto N, Fukushi D, Tominaga K, Kidokoro
644 H, Muramatsu Y, Nishi E, Nakamura S *et al*: **Phenotype-genotype correlations of**
645 **PIGO deficiency with variable phenotypes from infantile lethality to mild**
646 **learning difficulties**. *Hum Mutat* 2017, **38**(7):805-815.
- 647 37. Naseer MI, Rasool M, Jan MM, Chaudhary AG, Pushparaj PN, Abuzenadah AM, Al-
648 Qahtani MH: **A novel mutation in PGAP2 gene causes developmental delay,**
649 **intellectual disability, epilepsy and microcephaly in consanguineous Saudi family**.
650 *J Neurol Sci* 2016, **371**:121-125.
- 651 38. Abdel-Hamid MS, Issa MY, Otaify GA, Abdel-Ghafar SF, Elbendary HM, Zaki MS:
652 **PGAP3-related hyperphosphatasia with mental retardation syndrome: Report of**
653 **10 new patients and a homozygous founder mutation**. *Clin Genet* 2017.
- 654 39. Pagnamenta AT, Murakami Y, Taylor JM, Anzilotti C, Howard MF, Miller V,
655 Johnson DS, Tadros S, Mansour S, Temple IK *et al*: **Analysis of exome data for 4293**
656 **trios suggests GPI-anchor biogenesis defects are a rare cause of developmental**
657 **disorders**. *Eur J Hum Genet* 2017, **25**(6):669-679.
- 658 40. Nampoothiri S, Hebbar M, Roy AG, Kochumon SP, Bielas S, Shukla A, Girisha KM:
659 **Hyperphosphatasia with Mental Retardation Syndrome Due to a Novel Mutation**
660 **in PGAP3**. *J Pediatr Genet* 2017, **6**(3):191-193.

- 661 41. Hoglebe M, Murakami Y, Wild M, Ahlmann M, Biskup S, Hortnagel K, Gruneberg
662 M, Reunert J, Linden T, Kinoshita T *et al*: **A novel mutation in PIGW causes**
663 **glycosylphosphatidylinositol deficiency without hyperphosphatasia.** *Am J Med*
664 *Genet A* 2016, **170**(12):3319-3322.
- 665 42. Belet S, Fieremans N, Yuan X, Van Esch H, Verbeeck J, Ye Z, Cheng L, Brodsky BR,
666 Hu H, Kalscheuer VM *et al*: **Early frameshift mutation in PIGA identified in a**
667 **large XLID family without neonatal lethality.** *Hum Mutat* 2014, **35**(3):350-355.
- 668 43. Swoboda KJ, Margraf RL, Carey JC, Zhou H, Newcomb TM, Coonrod E, Durtschi J,
669 Mallempati K, Kumanovics A, Katz BE *et al*: **A novel germline PIGA mutation in**
670 **Ferro-Cerebro-Cutaneous syndrome: a neurodegenerative X-linked epileptic**
671 **encephalopathy with systemic iron-overload.** *Am J Med Genet A* 2014, **164A**(1):17-
672 28.
- 673 44. Tarailo-Graovac M, Sinclair G, Stockler-Ipsiroglu S, Van Allen M, Rozmus J, Shyr C,
674 Biancheri R, Oh T, Sayson B, Lafek M *et al*: **The genotypic and phenotypic**
675 **spectrum of PIGA deficiency.** *Orphanet J Rare Dis* 2015, **10**:23.
- 676 45. Kim YO, Yang JH, Park C, Kim SK, Kim MK, Shin MG, Woo YJ: **A novel PIGA**
677 **mutation in a family with X-linked, early-onset epileptic encephalopathy.** *Brain*
678 *Dev* 2016, **38**(8):750-754.
- 679 46. Joshi C, Kolbe DL, Mansilla MA, Mason S, Smith RJ, Campbell CA: **Ketogenic diet**
680 **- A novel treatment for early epileptic encephalopathy due to PIGA deficiency.**
681 *Brain Dev* 2016, **38**(9):848-851.
- 682 47. Ohba C, Okamoto N, Murakami Y, Suzuki Y, Tsurusaki Y, Nakashima M, Miyake N,
683 Tanaka F, Kinoshita T, Matsumoto N *et al*: **PIGN mutations cause congenital**
684 **anomalies, developmental delay, hypotonia, epilepsy, and progressive cerebellar**
685 **atrophy.** *Neurogenetics* 2014, **15**(2):85-92.
- 686 48. Brady PD, Moerman P, De Catte L, Deprest J, Devriendt K, Vermeesch JR: **Exome**
687 **sequencing identifies a recessive PIGN splice site mutation as a cause of**
688 **syndromic congenital diaphragmatic hernia.** *Eur J Med Genet* 2014, **57**(9):487-
689 493.
- 690 49. Couser NL, Masood MM, Strande NT, Foreman AK, Crooks K, Weck KE, Lu M,
691 Wilhelmsen KC, Roche M, Evans JP *et al*: **The phenotype of multiple congenital**
692 **anomalies-hypotonia-seizures syndrome 1: report and review.** *Am J Med Genet A*
693 2015, **167A**(9):2176-2181.
- 694 50. Nakagawa T, Taniguchi-Ikeda M, Murakami Y, Nakamura S, Motooka D, Emoto T,
695 Satake W, Nishiyama M, Toyoshima D, Morisada N *et al*: **A novel PIGN mutation**
696 **and prenatal diagnosis of inherited glycosylphosphatidylinositol deficiency.** *Am J*
697 *Med Genet A* 2016, **170A**(1):183-188.
- 698 51. McInerney-Leo AM, Harris JE, Gattas M, Peach EE, Sinnott S, Dudding-Byth T,
699 Rajagopalan S, Barnett CP, Anderson LK, Wheeler L *et al*: **Fryns Syndrome**
700 **Associated with Recessive Mutations in PIGN in two Separate Families.** *Hum*
701 *Mutat* 2016, **37**(7):695-702.
- 702 52. Fleming L, Lemmon M, Beck N, Johnson M, Mu W, Murdock D, Bodurtha J,
703 Hoover-Fong J, Cohn R, Bosemani T *et al*: **Genotype-phenotype correlation of**
704 **congenital anomalies in multiple congenital anomalies hypotonia seizures**
705 **syndrome (MCAHS1)/PIGN-related epilepsy.** *Am J Med Genet A* 2016,
706 **170A**(1):77-86.
- 707 53. Khayat M, Tilghman JM, Chervinsky I, Zalman L, Chakravarti A, Shalev SA: **A**
708 **PIGN mutation responsible for multiple congenital anomalies-hypotonia-seizures**
709 **syndrome 1 (MCAHS1) in an Israeli-Arab family.** *Am J Med Genet A* 2016,
710 **170A**(1):176-182.

- 711 54. Nakashima M, Kashii H, Murakami Y, Kato M, Tsurusaki Y, Miyake N, Kubota M,
712 Kinoshita T, Saitsu H, Matsumoto N: **Novel compound heterozygous PIGT**
713 **mutations caused multiple congenital anomalies-hypotonia-seizures syndrome 3.**
714 *Neurogenetics* 2014, **15**(3):193-200.
- 715 55. Lam C, Golas GA, Davids M, Huizing M, Kane MS, Krasnewich DM, Malicdan
716 MCV, Adams DR, Markello TC, Zein WM *et al*: **Expanding the clinical and**
717 **molecular characteristics of PIGT-CDG, a disorder of**
718 **glycosylphosphatidylinositol anchors.** *Mol Genet Metab* 2015, **115**(2-3):128-140.
- 719 56. Skauli N, Wallace S, Chiang SC, Baroy T, Holmgren A, Stray-Pedersen A, Bryceson
720 YT, Stromme P, Frengen E, Misceo D: **Novel PIGT Variant in Two Brothers:**
721 **Expansion of the Multiple Congenital Anomalies-Hypotonia Seizures Syndrome 3**
722 **Phenotype.** *Genes (Basel)* 2016, **7**(12).
- 723 57. Kohashi K, Ishiyama A, Yuasa S, Tanaka T, Miya K, Adachi Y, Sato N, Saitsu H,
724 Ohba C, Matsumoto N *et al*: **Epileptic apnea in a patient with inherited**
725 **glycosylphosphatidylinositol anchor deficiency and PIGT mutations.** *Brain and*
726 *Development* 2017.
- 727 58. Xiong ZQ, Qian W, Suzuki K, McNamara JO: **Formation of complement**
728 **membrane attack complex in mammalian cerebral cortex evokes seizures and**
729 **neurodegeneration.** *The Journal of neuroscience : the official journal of the Society*
730 *for Neuroscience* 2003, **23**(3):955-960.
- 731 59. Maydan G, Noyman I, Har-Zahav A, Neriah ZB, Pasmanik-Chor M, Yehekel A,
732 Albin-Kaplanski A, Maya I, Magal N, Birk E *et al*: **Multiple congenital anomalies-**
733 **hypotonia-seizures syndrome is caused by a mutation in PIGN.** *J Med Genet* 2011,
734 **48**(6):383-389.
- 735 60. Horn D, Schottmann G, Meinecke P: **Hyperphosphatasia with mental retardation,**
736 **brachytelephalangy, and a distinct facial gestalt: Delineation of a recognizable**
737 **syndrome.** *European journal of medical genetics* 2010, **53**(2):85-88.
- 738 61. Ihara S, Nakayama S, Murakami Y, Suzuki E, Asakawa M, Kinoshita T, Sawa H:
739 **PIGN prevents protein aggregation in the endoplasmic reticulum independently**
740 **of its function in the GPI synthesis.** *J Cell Sci* 2017, **130**(3):602-613.
- 741 62. Ferry Q, Steinberg J, Webber C, FitzPatrick DR, Ponting CP, Zisserman A, Nellaker
742 C: **Diagnostically relevant facial gestalt information from ordinary photos.** *Elife*
743 2014, **3**:e02020.
- 744 63. Thompson MD, Nezarati MM, Gillesen-Kaesbach G, Meinecke P, Mendoza-
745 Londono R, Mornet E, Brun-Heath I, Squarcioni CP, Legeai-Mallet L, Munnich A *et*
746 *al*: **Hyperphosphatasia with seizures, neurologic deficit, and characteristic facial**
747 **features: Five new patients with Mabry syndrome.** *Am J Med Genet A* 2010,
748 **152A**(7):1661-1669.
- 749 64. Ng BG, Hackmann K, Jones MA, Eroshkin AM, He P, Williams R, Bhide S, Cantagrel
750 V, Gleeson JG, Paller AS *et al*: **Mutations in the Glycosylphosphatidylinositol**
751 **Gene PIGL Cause CHIME Syndrome.** *American journal of human genetics* 2012,
752 **90**(4):685-688.
- 753 65. Almeida AM, Murakami Y, Layton DM, Hillmen P, Sellick GS, Maeda Y, Richards
754 S, Patterson S, Kotsianidis I, Mollica L *et al*: **Hypomorphic promoter mutation in**
755 **PIGM causes inherited glycosylphosphatidylinositol deficiency.** *Nature medicine*
756 2006, **12**(7):846-851.
- 757 66. Davis EM, Kim J, Menasche BL, Sheppard J, Liu X, Tan AC, Shen J: **Comparative**
758 **Haploid Genetic Screens Reveal Divergent Pathways in the Biogenesis and**
759 **Trafficking of Glycophosphatidylinositol-Anchored Proteins.** *Cell Rep* 2015,
760 **11**(11):1727-1736.

- 761 67. Muniz M, Riezman H: **Trafficking of glycosylphosphatidylinositol anchored**
762 **proteins from the endoplasmic reticulum to the cell surface.** *Journal of lipid*
763 *research* 2016, **57**(3):352-360.
764